

# Destruction of Strong Critical Spin Fluctuations by Doping in the 2D Hubbard Model

Bumsoo Kyung

*Max Planck Institute for Physics of Complex Systems, Noethnitzer Str. 38, 01187 Dresden, Germany*  
(23 January 1998)

We present the doping dependence of the spectral functions, density of states and low frequency behavior of the self-energy for the 2D Hubbard model on the basis of our recently developed theory for the Hubbard model. Strong 2D critical spin fluctuations dominating near half-filling are completely destroyed by 13 and 20 % doping concentrations for  $U = 4$  and 8, respectively. Below these concentrations the imaginary part of the self-energy vanishes quadratically in frequency near the Fermi energy, a characteristic feature for the Fermi liquid.

PACS numbers: 71.10.Fd, 71.27.+a

High  $T_c$  superconductors found in cuprates have exhibited a rich phase diagram in doping ( $x = 1 - n$ ) and temperature ( $T$ ) plane [1]. At half-filling the materials are antiferromagnetic insulators over a wide range of temperature up to 200-300 K, and away from half-filling antiferromagnetic long-range order is destroyed by 2-3 % doping and further doping makes the cuprates be metallic and eventually superconducting. Right after the discovery of high  $T_c$  superconductors, the Hubbard model was proposed by Anderson [2] as the simplest model which might be able to describe the rich and anomalous phase diagram in the copper oxides. Although it was solved exactly in one-dimension [3], the exact solution in more than 2-dimensions is not known yet. Nonetheless, there is increasing numerical evidence [4,5] that for a half-filled 2D band, the  $T = 0$  ground state is antiferromagnetic insulating for all  $U$ , while at finite temperatures strong fluctuations destroy long-range antiferromagnetic order due to the Mermin-Wagner theorem [6]. Away from half-filling, however, there have been lack of reliable studies on the systematic change of dynamical properties by doping which include, particularly, the low frequency behavior of the self-energy.

Although quantum Monte Carlo (QMC) calculations [4,7,8] have exhibited the systematic change of the spectral properties away from half-filling in the 2D Hubbard model, the lack of a reliable method for numerical analytical continuation from QMC data containing inherent statistical errors as well as finite size effect have hindered a detailed study of some dynamical quantities such as the single particle self-energy. While there have been extensive studies on the low frequency behavior of the self-energy within fluctuation exchange (FLEX) approximation [9], 2D critical spin fluctuations are not properly taken into account in FLEX approximation. As a result, the scattering rates are linear (in frequency) over a wide range of frequency, but they always vanish quadratically near the Fermi energy for any available doping concen-

trations within FLEX.

Recently we formulated a theory to the 2D Hubbard model in a manner free of finite size effect and numerical analytical continuation, yet containing the essential features of the 2D Hubbard model, i.e., the correct atomic limit at large  $\omega$  and 2D spin fluctuations [10]. In this previous work for a half-filled 2D band, 2D critical spin fluctuations are found to give rise to a strong local maximum at the Fermi energy in the scattering rates for low temperatures, leading to a pseudogap in the spectral function. At zero temperature they are expected to yield eventually an antiferromagnetic insulating state. Therefore, an important and natural question away from half-filling is whether strong 2D critical spin fluctuations are destroyed by doping or not, and if it is the case, how and at which doping concentration electrons lose their strong correlations, eventually leading to a Fermi liquid-like behavior. In this Letter, we would like to answer this one of the central issues in the high  $T_c$  superconductivity for the first time.

In order to take into account strong 2D critical fluctuations properly, we impose the following three exact sumrules to the spin, charge, and particle-particle susceptibilities [10,11]:

$$\begin{aligned} \frac{T}{N} \sum_q \chi_{sp}(q) &= n - 2\langle n_{\uparrow}n_{\downarrow} \rangle \\ \frac{T}{N} \sum_q \chi_{ch}(q) &= n + 2\langle n_{\uparrow}n_{\downarrow} \rangle - n^2 \\ \frac{T}{N} \sum_q \chi_{pp}(q) &= \langle n_{\uparrow}n_{\downarrow} \rangle. \end{aligned} \quad (1)$$

$T$  and  $N$  are the absolute temperature and number of lattice sites.  $q$  is a compact notation for  $(\vec{q}, i\nu_n)$  where  $i\nu_n$  are either Fermionic or Bosonic Matsubara frequencies. The dynamical spin, charge and particle-particle susceptibilities are calculated by

$$\begin{aligned}
\chi_{sp}(q) &= \frac{2\chi_{ph}^0(q)}{1 - U_{sp}\chi_{ph}^0(q)} \\
\chi_{ch}(q) &= \frac{2\chi_{ph}^0(q)}{1 + U_{ch}\chi_{ph}^0(q)} \\
\chi_{pp}(q) &= \frac{\chi_{pp}^0(q)}{1 + U_{pp}\chi_{pp}^0(q)}.
\end{aligned} \tag{2}$$

$\chi_{ph}^0(q)$  and  $\chi_{pp}^0(q)$  are irreducible particle-hole and particle-particle susceptibilities, respectively, which are computed from

$$\begin{aligned}
\chi_{ph}^0(q) &= -\frac{T}{N} \sum_k G^0(k-q)G^0(k) \\
\chi_{pp}^0(q) &= \frac{T}{N} \sum_k G^0(q-k)G^0(k),
\end{aligned} \tag{3}$$

where  $G^0(k)$  is the noninteracting Green's function.  $U_{sp}$ ,  $U_{ch}$ , and  $U_{pp}$  in Eq. 2 are renormalized interaction constants for each channel which are calculated self-consistently by making an ansatz  $U_{sp} \equiv U \langle n_{\uparrow} n_{\downarrow} \rangle / (\langle n_{\uparrow} \rangle \langle n_{\downarrow} \rangle)$  [11] in Eq. 1. By defining  $U_{sp}$ ,  $U_{ch}$ , and  $U_{pp}$  this way, the Mermin-Wagner theorem as well as correct atomic limit for large  $\omega$  are satisfied simultaneously [10]. In order to find the chemical potential for interacting electrons, first we calculate Eqs. (1)-(3) and the self-energy (Eqs. (1) in Ref. [10]) with the noninteracting Green's function whose noninteracting chemical potential gives a desired electron concentration. Then, the chemical potential for interacting electrons is determined in such a way that the calculated electron concentration with the interacting Green's function is the same as the desired value. Throughout the calculations the unit of energy is  $t$  and all energies are measured from the chemical potential  $\mu$ . We used a  $128 \times 128$  lattice in momentum space and performed the calculations by means of well-established fast Fourier transforms (FFT). It should be also noted that we used a real frequency formulation in Eqs. (1)-(3) to avoid any possible uncertainties associated with numerical analytical continuation.

We start in Fig. 1 by studying the single particle spectral functions for  $U = 4$  at  $n = 1.0$ ,  $T = 0.05$  (Fig. 1(a)) and at  $n = 0.87$ ,  $T = 0.005$  (Fig. 1(b)). Within our numerical calculations, we do not have the self-consistent solution for  $U_{sp}$  at lower temperatures than 0.05 near half-filling. Note that the spin-spin correlation length exponentially increases like  $\xi \sim \exp(\text{constant}/T)$  at low temperatures near half-filling. In Fig. 1(a) for a half-filled band, a SDW pseudogap is open at the Fermi energy along the antiferromagnetic zone boundary and a small shadow structure is found in the opposite frequency side of the main peak at the other momenta. At  $n = 0.87$  (Fig. 1(b)), generally the spectral weight is transferred near the Fermi energy and a shadow feature is strongly suppressed throughout the Brillouin zone. The spectral

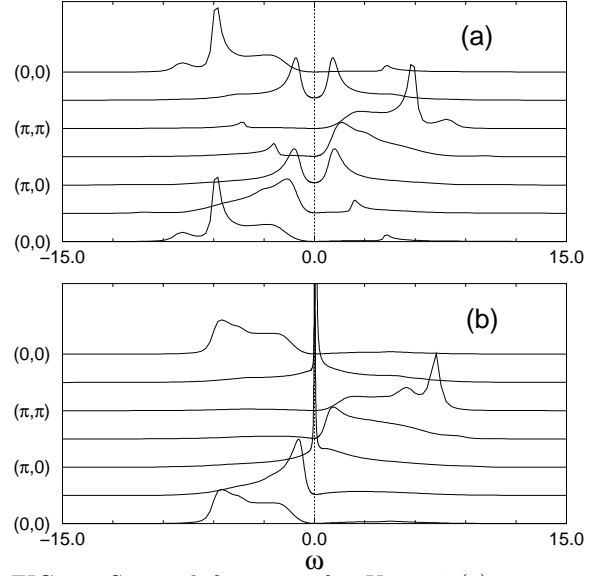


FIG. 1. Spectral functions for  $U = 4$  (a) at  $n = 1.0$ ,  $T = 0.05$  and (b) at  $n = 0.87$ ,  $T = 0.005$ .

functions along the antiferromagnetic zone boundary are so drastically changed at this electron concentration that the SDW pseudogap is completely closed and a sharp quasiparticle peak begins to develop near the Fermi energy.

In Fig. 2 we present the systematic change of the density of states and low frequency part of the self-energy by varying the electron concentration from  $n = 1.0$  to 0.95, 0.90 and 0.87. As the concentration is decreased, the spectral weight tends to move near the Fermi energy and to fill the SDW pseudogap (Fig. 2(a)). At  $n = 0.90$  (dotted curve), most of the SDW pseudogap is closed and a small peak develops at the Fermi energy. At  $n = 0.87$  (solid curve), the SDW pseudogap is completely destroyed by doping with the appearance of a narrow and sharp spectral weight at the Fermi energy. At this stage a Fermi liquid-like behavior is expected to set in. In Fig. 2(b) the low frequency part of the scattering rates is shown for the same parameters as in Fig. 2(a). At  $n = 1.0$  (dot-dashed curve), strong 2D critical spin fluctuations give rise to enormous scattering rates near the Fermi energy, eventually leading to an antiferromagnetic insulator at zero temperature. At  $n = 0.95$  (dashed curve), they are still persisting and shifted to the positive frequency side. At  $n = 0.90$  (dotted curve), most of the critical fluctuations are destroyed by doping with a small remnant in the positive frequency side. At  $n = 0.87$  (solid curve), the 2D critical fluctuations are completely washed out and the imaginary part of the self-energy vanishes quadratically in frequency near the Fermi energy, a characteristic feature for the Fermi liquid.

In Fig. 3 the single-particle spectral functions for  $U = 8$  at  $n = 1.0$ ,  $T = 0.05$  (Fig. 3(a)) and at  $n = 0.80$ ,  $T = 0.005$  (Fig. 3(b)) are shown. At  $n = 1.0$ , four

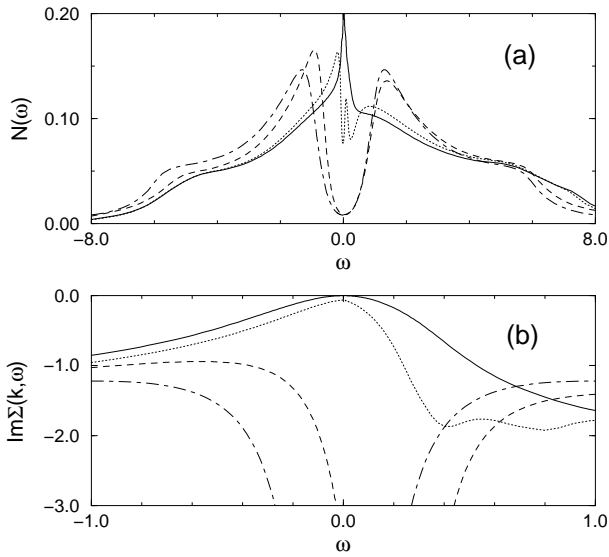


FIG. 2. (a) Density of states and (b) low frequency domain of the imaginary part of the self-energy at the noninteracting Fermi surface for  $U = 4$  at different electron concentrations  $n = 1.0, 0.95, 0.90$ , and  $0.87$  denoted as the dot-dashed, dashed, dotted, and solid curves, respectively. For  $n = 1.0$  and  $0.95$ ,  $T$  is  $0.05$ , while for  $n = 0.90$  and  $0.87$ ,  $T$  is  $0.005$ .

peaks are found in the spectral function, two peaks associated with the SDW bands near the Fermi energy and the other two with the Hubbard bands in the intermediate frequency regime. The Hubbard bands appear dispersionless since they arise from strong local repulsions, and for  $U = 8$  they are more pronounced than the SDW bands [10]. The SDW pseudogap is more visible along the antiferromagnetic zone boundary, but its total spectral weight is much more suppressed compared with that for  $U = 4$  in Fig. 1. At  $n = 0.80$  (Fig. 3(b)), the spectral weight is transferred near the Fermi energy throughout the Brillouin zone, as is the case for  $U = 4$  in Fig. 1(b). At this electron concentration, the Hubbard bands are strongly suppressed and their significant spectral weight moves near the Fermi energy to fill the SDW pseudogap. The sharp quasiparticle peaks appear near the Fermi energy.

The density of states and low frequency part of the scattering rates for  $U = 8$  at different electron concentrations from  $n = 1.0$  to  $0.91, 0.85$  and  $0.80$  are presented in Fig. 4. As the concentration is decreased, a considerable spectral weight associated with the Hubbard bands (Fig. 4(a)) moves near the Fermi energy and starts to fill the SDW pseudogap. At  $n = 0.85$  (dotted curve), most of the SDW pseudogap is closed and a small peak develops at the Fermi energy, as in Fig. 2(a). At  $n = 0.80$  (solid curve), the SDW pseudogap is completely closed by doping and a narrow, sharp spectral weight appears at the Fermi energy. In Fig. 4(b) the low frequency part of the scattering rates is also shown for the same parameters as in Fig. 4(a). At  $n = 1.0$  and  $0.91$  (dot-dashed and

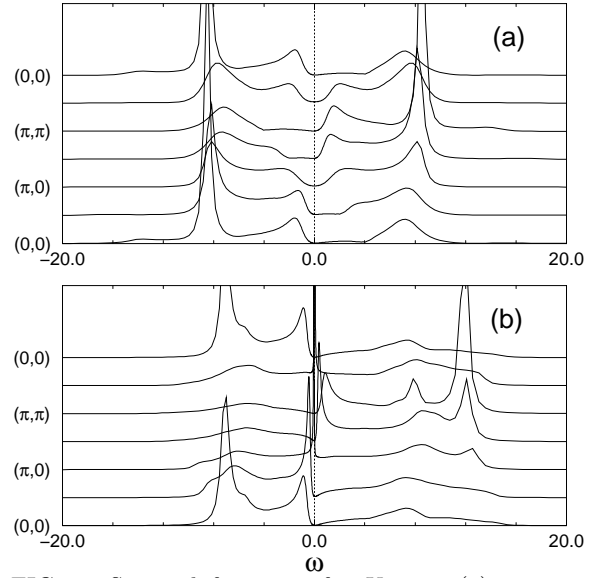


FIG. 3. Spectral functions for  $U = 8$  (a) at  $n = 1.0$ ,  $T = 0.05$  and (b) at  $n = 0.80$ ,  $T = 0.005$ .

dotted curves), strong 2D critical fluctuations are still dominating near the Fermi energy. At  $n = 0.85$  (dotted curve), most of the 2D critical fluctuations are already destroyed by doping with a small remnant. Eventually 20 % doping (solid curve) destroys the 2D critical fluctuations completely and the scattering rates approach zero quadratically in frequency near the Fermi energy, as in Fig. 2(b) for  $U = 4$ .

We plot in Fig. 5 the imaginary parts of the dynamical spin susceptibility for  $U = 8$  at  $n = 1.0$ ,  $T = 0.05$  (Fig. 5(a)) and at  $n = 0.80$ ,  $T = 0.005$  (Fig. 5(b)). Both cases in Fig. 5 show a similar behavior at small and intermediate momenta except that the maxima for the former occur at a smaller energy scale than that for the latter, consistent with the recent QMC calculations [8]. The most dramatic difference happens at  $\vec{q} = (\pi, \pi)$  (solid curves). For a half-filled 2D band (See the inset in Fig. 5(a)),  $\text{Im}\chi_{sp}(\vec{q}, \nu)$  shows a nearly divergent behavior at small frequencies (its maximum  $6760/t$  occurs at  $5.5 \times 10^{-5}t$ ), while at  $n = 0.80$  (Fig. 5(b))  $\text{Im}\chi_{sp}(\vec{q}, \nu)$  exhibits only a broad maximum at  $0.75t$ . This drastic change in  $\text{Im}\chi_{sp}(\vec{q}, \nu)$  is mainly responsible for the major differences discussed earlier for these two electron concentrations.

Before closing we comment on the low frequency behavior of the self-energy.  $\text{Im}\Sigma(\vec{k}, \omega)$  for  $U = 4$ ,  $n = 0.87$  and for  $U = 8$ ,  $n = 0.80$  are also examined on a much smaller energy scale from  $-0.1$  to  $0.1$  which is not shown in this Letter. The quadratic behavior is still found with a small constant shift (due to a finite temperature effect). For the former case, the scattering rates vanish as  $\omega^{1.95}$  near the Fermi energy, while for the latter as  $\omega^{1.94}$ . As is shown in Figs. 2 and 4, we do not also find any indication of a linear frequency dependence for the scattering

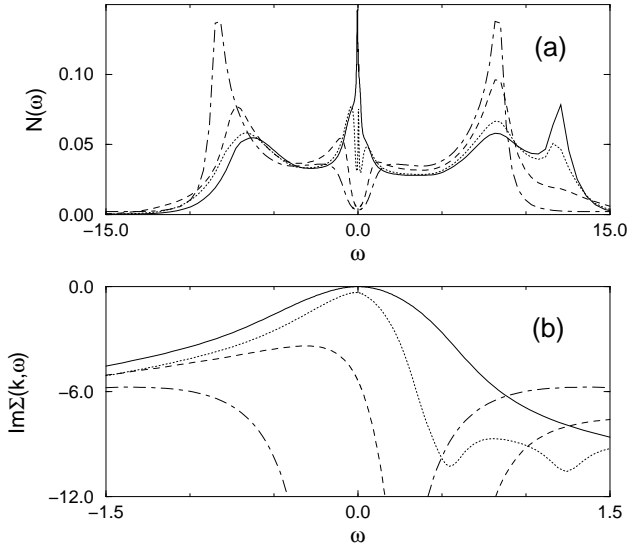


FIG. 4. (a) Density of states and (b) low frequency domain of the imaginary part of the self-energy at the noninteracting Fermi surface for  $U = 8$  at different electron concentrations  $n = 1.0, 0.91, 0.85$ , and  $0.80$  denoted as the dot-dashed, dashed, dotted, and solid curves, respectively. For  $n = 1.0$  and  $0.91$ ,  $T$  is  $0.05$ , while for  $n = 0.85$  and  $0.80$ ,  $T$  is  $0.005$ .

rates. Hence, as long as the 2D Hubbard model with only nearest neighbor hopping is concerned, our calculations do not show the frequency dependence of the scattering rates from FLEX approximation [9] or from the marginal Fermi liquid hypothesis [12].

In summary, the doping dependence of the spectral functions, density of states and low frequency behavior of the self-energy has been studied for the 2D Hubbard model based on our recently developed theory for the Hubbard model. Strong 2D critical spin fluctuations dominating near half-filling are completely destroyed by 13 and 20 % doping concentrations for  $U = 4$  and  $8$ , respectively. Below these concentrations the scattering rates vanish quadratically in frequency near the Fermi energy, a characteristic feature for the Fermi liquid.

The author would like to thank Prof. P. Fulde, and Drs. S. Blawid, R. Bulla, T. Dahm, P. Kornilovitch, M. Laad, W. Stephan and numerous other colleagues in the Max Planck Institute for Physics of Complex Systems for useful discussions.

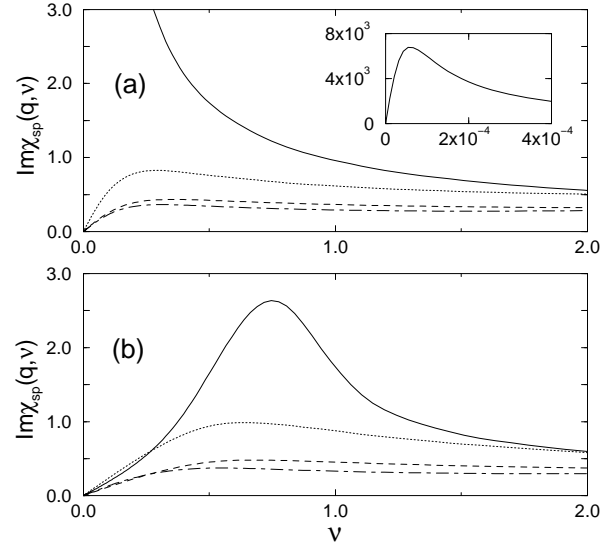


FIG. 5. Imaginary part of the dynamical spin susceptibility for  $U = 8$  (a) at  $n = 1.0$ ,  $T = 0.05$  and (b) at  $n = 0.80$ ,  $T = 0.005$ . The dot-dashed, dashed, dotted and solid curves denote  $\text{Im}\chi_{sp}(\vec{q}, \nu)$  at  $i = 1, 2, 3$  and  $4$  for  $\vec{q} = i(\pi/4, \pi/4)$ , respectively.

- [4] S. R. White, Phys. Rev. B **44**, 4670 (1991); M. Vekić and S. R. White, *ibid.* **47** 1160 (1993).
- [5] E. Dagotto, Rev. Mod. Phys. **66**, 763 (1994), and references therein.
- [6] N. D. Mermin and H. Wagner, Phys. Rev. Lett. **17**, 1133 (1966).
- [7] N. Bulut, D. J. Scalapino, and S. R. White, Phys. Rev. Lett. **72**, 705 (1994); *ibid.* **73**, 748 (1994).
- [8] R. Preuss, W. Hanke, and W. von der Linden, Phys. Rev. Lett. **75**, 1344 (1995); R. Preuss *et al.*, *ibid.* **79**, 1122 (1997).
- [9] T. Dahm and L. Tewordt, Phys. Rev. B **52**, 1297 (1995); S. Wermbter, *ibid.* **53**, 10 569 (1996); S. Wermbter, *ibid.* **55**, 10 149 (1997).
- [10] Bumsoo Kyung (unpublished).
- [11] Y. Vilk and A. M. Tremblay, to appear in J. Physics (Paris)(Nov.1997); cond-mat/9702188.
- [12] C. M. Varma *et al.*, Phys. Rev. Lett. **63**, 1996 (1989).

- 
- [1] C. Almasan and M. B. Maple in *Chemistry of High temperature Superconductors*, edited by C. N. R. Rao (World Scientific, Singapore, 1991).
  - [2] P. W. Anderson, Science **235**, 1196 (1987).
  - [3] E. H. Lieb and F. Y. Wu, Phys. Rev. Lett. **20**, 1445 (1968).